HHS Public Access

Author manuscript

Trends Biotechnol. Author manuscript; available in PMC 2018 November 01.

Published in final edited form as:

Trends Biotechnol. 2017 November ; 35(11): 1049–1061. doi:10.1016/j.tibtech.2017.08.008.

Computational Fluid Dynamics and Additive Manufacturing to Diagnose and Treat Cardiovascular Disease

Amanda Randles[a,b,*], **David H. Frakes**[b], and **Jane A. Leopold**[c]

[a]Duke University, Durham, NC, USA

[b]Arizona State University, Tempe, AZ

[c]Brigham and Women's Hospital, Boston, MA, USA

Abstract

Non-invasive engineering models are now being used for diagnosing and planning the treatment of cardiovascular disease. Techniques in computational modeling and additive manufacturing have matured concurrently, and results from simulations can inform and enable the design and optimization of therapeutic devices and treatment strategies. The emerging synergy between large-scale simulations and 3D printing is having a two-fold benefit: first, 3D printing can be used to validate the complex simulations, and second, the flow models can be used to improve treatment planning for cardiovascular disease. In this review, we summarize and discuss recent methods and findings for leveraging advances in both additive manufacturing and patient-specific computational modeling, with an emphasis on new directions in these fields and remaining open questions.

Keywords

computational fluid dynamics; high performance computing; additive manufacturing; cardiovascular disease; 3D printing

New strategies for modeling cardiovascular disease

Engineering modeling advances have played critical roles in the diagnosis and treatment of vascular disease since at least the 1990s when the first image-based modeling technologies were developed for simulating hemodynamics [1]. These models have provided non-invasive techniques for both diagnostics and treatment planning. The models can also be used to drive the development of therapeutic devices. The long-term utility of these models, however, is limited by the available computational power and validation capabilities. Two trends have emerged that warrant an exposition on the synergy between massively parallel hemodynamic simulations and additive manufacturing. First, three-dimensional printing can

*Corresponding author: amanda.randles@duke.edu (Amanda Randles).

be used to create phantoms and facilitate *in vitro* experiments to validate flow models using complex vascular geometries that recapitulate the vascular system *in vivo*. The construction of patient-specific geometric models from medical imaging data has enabled the precise identification of areas of perturbed blood flow and prediction of how flow patterns will change following possible therapeutic interventions. Second, high-resolution CFD simulations can be used to drive the development or refinement of medical devices by providing much needed information on the anatomic variations, biomechanical forces, and wall properties that can influence the design of stents, flow diverters, stent grafts and conduits, and similar devices. In this review, we concentrate on these two trends after we briefly describe the impact of **wall shear stress (WSS, see Glossary)** and affiliated computational techniques on the study and treatment of vascular disease, device design, and evaluation.

The Vascular System

The cardiovascular system is a highly integrated closed loop circuit of vessels that circulates blood to deliver oxygen and nutrients to organs and removes byproducts of metabolism. The vascular system exists in an arborized pattern with vessels and daughter branches arranged into vascular beds based on the end organ served. Within the vascular system, the cross-sectional area of the combined capillary beds is approximately 103 times greater than that of the aorta with a concomitant decrease in flow velocity as vessel diameter decreases [2]. Functional differences between vascular beds are attributable to both the structural properties of the vessels (i.e., vessel diameter, length, tortuosity, and stiffness) and the effects of hemodynamic forces on vascular phenotype. Blood vessels are continuously exposed to hemodynamic forces resulting from pulsatile pressure generated by cardiac contraction, the flow characteristics of circulating blood, and modifications to these forces locally by the geometry and mechanical properties of the blood vessels themselves [3].

Tensile stress and WSS are the key mechanical forces that regulate and maintain vascular homeostatic phenotype and function in a spatial and temporal manner. Tensile stress is distributed circumferentially around the vessel wall and is related to blood pressure, lumen radius, and wall thickness. Tensile stress regulates autocrine and paracrine signaling between blood vessel cells, mediates angiogenesis, and maintains the normal vascular phenotype [4, 5]. WSS is determined by the gradient of blood velocity at the vessel wall surface and is influenced by blood viscosity. In normal human arteries with pulsatile flow, WSS ranges from 1–5 Pa, whereas it is between 0.1–0.5 Pa in the venous system, which is characterized by minimal pulsatility [6]. Laminar blood flow with normal WSS protects the vascular endothelium, increases production of nitric oxide and prostacyclin, upregulates expression of the vasculoprotective transcription factors Krüppel-like factor 2 (KLF2) and nuclear factor erythroid 2-related factor 2 (Nrf2), and is important for barrier function, maintaining an antithrombotic surface, and regulating vascular tone [7–9].

The vascular system is adaptive and capable of growth and remodeling (G & R) throughout development, adulthood, and aging. Growth and remodeling in blood vessels are inherently coupled processes that incorporate vascular dynamics and hemodynamic forces, such as WSS. At baseline, the healthy vasculature is at homeostasis with stresses at ambient levels

that maintain the vessel wall and render G & R quiescent. A theory to explain G & R based on a constrained mixture model assumes that a blood vessel can respond to hemodynamic stress, undergo G & R, and return to its basal state by modulating the response of vascular smooth muscle cells [10–12]. Based on this theory, G & R has been studied in response to transient and sustained changes in hemodynamic and mechanical loads in models of the arterial system. The study showed that an artery can maintain homeostatic conditions over a range of pressure and flow and with a range of material properties, an effect that was dependent on prestretch of elastin and collagen. This study also determined that prestretch of collagen and elastin played a role in homeostasis, whereas material properties determined response time [13]. Similar work has been performed to study other clinically relevant vascular diseases, including an infrarenal aorta model to study expansion of aneurysms and vein grafts in response to increased pressure [14, 15].

Injury to the vascular system can cause maladaptive vascular remodeling and vascular dysfunction. Vascular abnormalities may also occur following prolonged high blood pressure, diabetes mellitus, hyperlipidemia, inflammation, drugs, or toxins that promote chemical and/or hemodynamic stress and cause architectural changes predicted by G & R that remodel the vessel and form atherosclerotic plaques. These vascular lesions that alter the topography of the vessel wall, in turn, effect changes in local WSS causing luminal narrowing in areas of low WSS or outward remodeling of blood vessels and aneurysm formation in areas of high WSS [9]. In patients with congenital heart disease, the unique hemodynamic and WSS profiles have a propensity to lead to (mal)adaptive vascular remodeling and dysfunction in patterns not observed normally. Patents with coarctation of the aorta have low levels of time-averaged WSS in the descending aorta that correlate with atherosclerotic plaque formation; repair of the coarctation with resection and end-to-end anastomosis was associated with elevated time-averaged WSS in the vicinity of residual narrowings, indicating that these treated patients are at risk for the development of atherosclerosis in unique locations because of the repair [16]. Patients with congenital biscupid aorta valves were also had increased aorta WSS compared with individuals with tricuspid aortic valves, suggesting that the WSS and hemodynamic flow patterns contribute to aortic dilatation in these patients [17].

Cardiovascular disease continues to be an urgent clinical problem affecting 92.1 million adults in the US, with a projected 43.9% having some form of the disease by 2030 (http://www.who.int/mediacentre/factsheets/fs317/en/). Worldwide, cardiovascular disease accounts for 31% of deaths annually and is a significant contributor to cardiovascular morbidity. Current methodologies to diagnose and determine the severity or significance of cardiovascular disease at the level of blood vessels include non-invasive imaging, e.g., **computed tomography angiography (CTA)** and invasive angiography. Invasive procedures enable a higher resolution visual assessment of the vessel lumen using **intravascular ultrasound (IVUS)** or **optical coherence tomography (OCT)** imaging; however, these methods describe only anatomy and provide limited information about local hemodynamic forces. Other invasive techniques that functionally assess luminal narrowing are guidewire-based technologies with high fidelity sensors that provide a low-resolution summed measure of pressure. As standalone technologies, none of the aforementioned imaging or pressure

measurement tools can provide complex high-resolution assessments of flow in the vasculature or predict how flow-related parameters will change with a standard therapeutic intervention. Computational and advanced manufacturing tools can bridge this gap, and, to date, they are becoming more widely employed in the diagnosis and treatment of vascular disease.

Computational Fluid Dynamics

The quantification of hemodynamic forces, including velocity and pressure fields on a per-patient basis is poised to play a crucial role in the diagnosis of, and treatment planning for, patients with cardiovascular disease. Understanding the principles that govern vascular disease localization and progression has been a long-established goal of computational biomechanics [18]. Models used to understand these principles have ranged from 0D to 3D numerical methods to represent the human vascular system. The 0D models, or lumped parameter models, include no spatial dimensions and assume physiological variables such as pressure and resistance to be spatially uniform across the system. 1D models can represent wave propagation and reflection and represent the physiological variables in one spatial dimension. Simulations in 2D often assume symmetry of the solution about a central axis. There are several excellent references on the broader spectrum of CFD models [19–22]. This review focuses on massively parallel 3D models of hemodynamics.

Figure 1 shows the process for deriving fluid and 3D printed models from medical imaging modalities. Methods for quantifying vascular flow start with deriving patient-specific anatomic and physiologic data from imaging modalities such as **computed tomography angiography (CTA)**, **magnetic resonance imaging (MRI)**, ultrasound, IVUS and OCT imaging. The medical images must resolve sufficient anatomical detail for segmentation and geometry extraction. Segmentation software is used to convert the medical images to a triangulated mesh based on the vascular anatomy. Table 1 provides a sample of popular segmentation packages for building the meshes that typically serve as input to the complex numerical solvers used in 3D CFD simulations. Withey and Koles detail an in depth review of the methods and available software for medical **image segmentation** [23]. Furthermore, PACS systems, such as eRAD Image Medical and Osirix, now offer a range of segmentation capabilities.

Blood flow within the vasculature is then simulated as an incompressible fluid. Flowing blood in the larger arteries can be represented as a Newtonian fluid, whereas the shear rates in smaller vessels necessitate a non-Newtonian description [24]. Table 2 provides an overview of current state-of-the-art computational hemodynamic software packages.

As modeling the entire vascular system is not tractable, the simulated region will include at least one inlet and one outlet where physiological boundary conditions must be specified. These conditions are typically based on either data measured for a specific patient, average patient data, a physical model, or defined assumptions. The challenge lies in patient-specific tuning of the boundary conditions. These conditions can be specified by setting the pressure or flow at the boundaries or by coupling an additional, lower-order model to the 3D CFD solver to provide more realistic conditions. The coupled models enable detailed analysis in

the 3D region while providing efficient models of regions proximal and distal to the area of interest [22]. Furthermore, lumped parameter and coupled models can account for wave propagation phenomena present in the arteries. The proper choice of boundary conditions influences the robustness, stability, computational cost, and accuracy of 3D simulations [25, 26]. To match clinical data, parameter estimation, automated tuning, and uncertainty quantification are often necessary [27–29].

Typically, such large-scale models rely on either a **Navier-Stokes** [30] or **lattice Boltzmann** solver [31, 32]. The computational demands of these simulations have historically restricted their size and scope, but advances in parallel algorithms and computer hardware have extended the reach of these simulations to much larger regions [30, 32–34]. **High-performance computing (HPC)** has extended the time-scale, domains, and fidelity that can be captured with CFD simulations. Efforts to simulate the full arterial network of the human body have started to be undertaken. In 2013, Xiao and colleagues completed a key feasibility study for simulating flow in a full body simulation [35]. The largest 3D simulation to date simulated flow in all arteries of a human greater than 1 mm in diameter [34]. The flow was simulated at a 9 μm resolution, required 509 billion grid points, and was modeled using 1.6 million processors. Example results from a parallel CFD simulation are shown in Figure 2, depicting different types of data that can be extracted: pressure, velocity streamlines, and wall shear stress. Other key challenges to accurately representing patient-specific hemodynamics are capturing the material properties of the vessel walls and, sometimes, explicitly accounting for cells in the blood. Typically for fluid structure interaction (FSI), the fluid domain will be coupled to the solid domain using a momentum coupling in which the wall or cells are models as elastic materials. FSI models are necessary to simulate study of the role of ventricular and valve hemodynamics [36, 37]. As outlined in Table 2, many of the aforementioned CFD software packages have begun building in FSI capabilities. Traditional FSI techniques rely on the arbitrary Lagrangian-Eulerian (ALE) method, and, more recently, alternatives such as the coupled momentum method (CMM) and immersed boundary method (IBM) are becoming popular [21]. In each case, stability concerns must be addressed and vessel-specific properties are needed to parameterize the model.

A key goal for CFD studies is to provide insight into the relationships between vascular anatomy, local hemodynamics, and the development and progression of vascular disease and, thereby, serve as a diagnostic tool. Understanding the connection between flow patterns and topology is particularly important for simulations using geometries derived from medical imaging data. CFD enables non-invasive capture of critical hemodynamic variables from a study intended to provide anatomical information only. The importance of these hemodynamic variables has been realized over the last few decades, with the identification of parameters such as low or oscillatory WSS [38, 39], pressure gradients [40], and velocity flow fields [41] as risk factors for both different vascular diseases and mechanobiologic drivers of vascular growth, remodeling, and adaptation. Large computational studies investigating the use of such hemodynamic markers in diagnosis have been completed for a range of diseases including but not limited to coarctation of the aorta [16, 42, 43], atherosclerosis [32, 44, 45], aortic aneurysms [46–48], cerebral aneurysms [49–51],

coronary artery bypass grafting (CABG) [52], Kawasaki disease [53] (D. Sengupta, PhD thesis, University of California-San Diego, 2013), and congenital heart diseases [54–57].

Three-dimensional hemodynamic simulations are approaching widespread use for the diagnosis of cardiovascular disease. The use of CFD for clinical decision support is increasing [58]. In 2014, the FDA approved the Heartflow FFR-CT software, which enables physicians to non-invasively evaluate hemodynamics in the coronary arteries and determine the functional severity of a blockage based on a quantity known as **fractional flow reserve (FFR)** [59]. Prior to the availability of this service, FFR could be obtained only through invasive testing.

3D Printing

3D printing is a process of additive manufacturing by which a 3D object is built layer-by-layer. The process is fundamentally different from subtractive manufacturing, wherein a 3D object is formed by progressively cutting material away from a solid block (e.g., computer numerical control, or CNC, cutting). The clear advantage of 3D printing is that the process can be applied to create arbitrarily complex geometries, whereas geometries created through subtractive manufacturing must be compatible with the limited access afforded to cutting tools operating from the outside in. Different 3D printing technologies relevant to the biomedical field include stereolithography, fused deposition modeling, digital light processing, and selective laser sintering, among others.

Studies of flow in 3D printed models necessarily require coupling with a flow measurement system. One option is MRI, which can measure flows within models printed directly by machines including the Objet family (Stratasys, Eden Prairie, MN, USA) [60]. Another option is **particle image velocimetry (PIV)**, which, unlike MRI, requires optical access to the flow test section. Directly printed models for PIV flow experiments have been used for decades [61]. However, the process is challenged by the inherent layering artifacts generated by 3D printing. These artifacts can disturb refractive index uniformity within a model, even when accessed from only a certain direction (e.g., a direction in-plane with respect to the created layers). The artifacts may also disrupt fluid mechanics near the boundary layer in the form of small-scale recirculation. When applying PIV to test sections representing anatomical geometries, the best overall results we observed were generated by more industrial grade PIV systems (e.g., the LaVision Flowmaster system (LaVision, Ypsilanti, MI, USA)) in conjunction with models that were recast using a 3D print as the starting point [62]. Figure 3 shows an example setup. One process for generating these models begins with 3D printing a core model out of wax using a Solidscape MAX2 printer (Solidscape, Merrimack, NH, USA). Investment plaster is then used to form a mold around the core, and the core is dissolved out. Next, a eutectic metal core can be recast inside the mold, and the mold is then removed. Lastly, a transparent material such as urethane or silicone can be poured and set around the metallic core, and the core is subsequently melted out, leaving a transparent lost-core model suitable for PIV. This process enables management of interior surface smoothness during the recasting process. Further, despite the optical requirements of PIV, such models can be used in conjunction with metallic medical devices that tend to disrupt MR imaging.

The aforementioned method is, of course, only one of numerous viable mechanisms for 3D printing vascular models for flow experiments or otherwise. Most popular among these other mechanisms may be the Objet family of devices mentioned earlier in the context of MRI-based experiments. As demonstrated in [63] and [64], this platform can generate highly accurate vascular models at the scale of the human neurovasculature. Compared with the originally segmented and reconstructed (virtual) anatomy in [64], high-resolution CT scans of the 3D printed anatomy provided (virtual) 3D models that differed on the order of only 100 microns based on distance analysis. Table 3 lists other forms of additive manufacturing.

Treatment Planning and Device Design

3D Printing vasculature for education

3D printing has been applied extensively in the context of cardiovascular disease for educating students, patients, and families [65, 66], and for treatment planning [67, 68]. 3D prints of relevant cardiovascular anatomy are typically generated based on the same types of medical images used to construct 3D geometries for CFD analyses (e.g., CT, MRI, angiography, IVUS, etc.). For treatment planning, both anatomical and physiological (e.g., blood flow) representations of cardiovascular structures have been targeted as end points. For example, in repair planning, the use of anatomical representations of congenital heart defects or other structural heart disease is growing rapidly. Ryan and colleagues [68] demonstrated models printed with a 3D Systems Zprinter 650 machine (3D Systems, Rock Hill, SC, USA) that communicated cardiovascular anatomy and associated anomalies through specific colorization. Other models such as those produced by Costello and colleagues enable surgical practice of the repair procedure [69]. Such models can be fabricated using the Objet family of printers (Stratasys, Eden Prairie, MN, USA) or similar machines.

Validating patient-specific fluid simulations through comparison with results from in vitro experiments

Additive manufacturing in combination with experimental techniques such as PIV is being used to validate CFD simulations in complex geometries. Traditionally, CFD packages were validated through comparison with analytical results [70, 71]. Such comparisons become untenable for complex geometries such as those found in the human vasculature. Some work has compared fluid simulation results with *in vivo* measurements from 4D-MRI [72, 73]; however, it is nearly impossible to control input parameters in a living biological system. 3D printed models offer a method to perform controlled fluid experiments for simulation validation. Such validation studies have been completed for aortic flow [43], cerebral aneurysms [50, 62], valve/leaflet interaction [74], coronary artery disease [32, 75–79], CABG [52, 80, 81] and in a left ventricular assist device (LVAD) [82]. An iterative feedback loop can be established to optimize the fluid simulations and ensure reproducible, robust, and accurate results. Figure 4 shows an example comparison between fluid simulation and experimental results.

Comparisons of simulation results with experimental results provide a critically valuable mechanism toward ensuring that simulations are, in fact, realistic. However, one persistent

challenge in authentically recreating *in vivo* environments *in vitro* is building vascular phantoms that behave physiologically with respect to fluid structure interaction. Vascular phantoms with a range of Young's moduli and Shore hardnesses that overlap with *in vivo* conditions can be 3D printed (and/or recast after 3D printing), but isolating the vascular geometry in the laboratory, and thereby omitting the many surrounding structures and dynamics present *in vivo*, necessarily limits the degree to which *in vivo* conditions can be reproduced. The ability to recapitulate *in vivo* conditions both anatomically and mechanically remains a relatively unsolved problem.

Leveraging CFD simulations to inform treatment planning and device design

The results of the fluid simulations can also be used to refine the 3D printed model most often for treatment planning and device design. Through fluid simulations, many perturbations of device designs or treatment options can be simulated *in silico* before either high cost surgery or further *in vitro* experiments. CFD simulations have been used to evaluate the design of Y-grafts for Fontan operations [83–85], anastomosis design [86], stents [87, 88], and flow-diverters [89, 90]. To enable predictive treatment planning, the mesh representing the vascular geometry is modified to represent different potential surgical outcomes. This approach of using 3D flow simulations to interrogate and optimize treatment plans has been used successfully for cerebral aneurysms [91, 92], coarcted aortas [93, 94], and other congenital disorders [95].

Concluding Remarks

The advancement of both high performance computing and 3D printing has presented a unique opportunity to tackle key questions in vascular biology at unprecedented scale and complexity. The trends toward patient-specific computational simulations and models have necessitated the ability to validate flow in such complex models, enabling high-resolution diagnostic screens, new techniques to predict the outcome of different treatment options, and improved device design. We propose that the synergy between large-scale hemodynamic simulation and 3D printing will transform development and treatment of vascular disease. However, many open challenges remain (see Outstanding Questions). We expect that patient-specific modeling (both experimental and computational) will produce a quantitative method for more accurate diagnostics and treatment on a per-patient basis.

Outstanding Questions

What data analyses will be needed to quantitatively assess a wide range of treatment options?

What are the limits in terms of scale and resolution that we can 3D print biocompatible medical devices? What computational limits must be overcome to facilitate near real-time diagnostics? What computational limits must be overcome to enable patient-specific device design and manufacturing?

What analytical methods can be used to extend the temporal domain captured by high-resolution CFD models?

How do we address the need for parameter estimation, automated tuning to match clinical data, and uncertainty quantification in cardiovascular simulations?

Can we capture flow in large regions of the human vasculature that include cellular components such as erythrocytes and neutrophils in computationally tractable simulations?

How do we build fully integrated models of cardiac function, ventricular hemodynamics, and valves in a data-driven, computationally efficient manner?

How can we 3D print vascular phantoms that are not only anatomically accurate but also physiologically accurate?

Acknowledgments

The work reported in this publication was supported by the Office Of The Director, National Institutes Of Health under Award Number DP5OD019876 and NIH/NHLBI U01 HL125215. The content is solely the responsibility of the authors and does not necessarily represent the official views of the National Institutes of Health. This material is also based upon work supported by the National Science Foundation under Grant No. 1512553. The authors thank Justin Ryan from Phoenix Children's Hospital for his assistance and Howard Fried for his feedback and comments.

Glossary

3D printing
a process of additive manufacturing by which a 3D object is built layer-by-layer.

Computational fluid dynamics (CFD)
numerical analysis used to solve fluid dynamics equations and simulate flow in complex geometries.

Computed tomography angiography (CTA)
anon-invasive imaging study that uses an injection of iodinated contrast to visualize blood vessels.

Fractional flow reserve (FFR)
this measurement accounts for the pressure gradient across a narrowed region in an artery. It is typically measured using an invasive, guide-wire based catheter procedure.

High performance computing (HPC)
massively parallel computing has been leveraged in recent years to extend the domain, time-scale, and resolution of CFD simulations. HPC relies on the use of large-scale parallel systems typically with more than one thousand processors.

Lattice Boltzmann method
an alternative approach to solving the standard Navier-Stokes equations governing fluid motion. It is based on kinetic theory and represents the fluid as a probability distribution function of particles that can move at discrete velocities around fixed Cartesian lattice.

Image segmentation

the process of partitioning an image from a medical imaging modality into different segments. Typically, in the case of studying vascular phenomena, the vessel lumen is extracted in a 3D stack of images. The extracted vessel walls are then stitched together to create a 3D triangulated mesh depicting a patient's vascular topology. The goal of segmentation is to create a representation that can be used as input for 3D printing or simulation.

Intravascular ultrasound (IVUS)
a miniature ultrasound probe attached to the tip of a catheter that is placed inside a blood vessel and provides images of a vessel lumen and vessel wall.

Navier-Stokes equations
physical models used to capture the motion of fluids that are derived from Newton's second law of motion. They are the common equations underlying computational fluid dynamics simulations.

Optical coherence tomography (OCT)
a catheter-based intravascular imaging technique that uses light scattering to image blood vessels with ultrahigh resolution (10 microns).

Particle-image-velocimetry (PIV)
an experimental technique to optically measure flow patterns.

Magnetic resonance imaging (MRI)
a non-invasive study that creates high-resolution images of structures in the body using a magnetic field, pulse radio wave energy, and field gradients.

Wall shear stress (WSS)
the stress that the fluid applies to the vessel wall, a known pathogenic factor in a range of vascular diseases.

References

1. Taylor CA, Figueroa C. Patient-specific modeling of cardiovascular mechanics. Annual review of biomedical engineering. 2009; 11:109–134.
2. Sherwood, L. Fundamentals of human physiology. Cengage Learning; 2011.
3. Secomb TW. Hemodynamics. Comprehensive Physiology. 2016
4. Qu MJ, Liu B, Wang HQ, Yan ZQ, Shen BR, Jiang ZL. Frequency-dependent phenotype modulation of vascular smooth muscle cells under cyclic mechanical strain. Journal of vascular research. 2007; 44(5):345–353. [PubMed: 17713348]
5. Yung YC, Chae J, Buehler MJ, Hunter CP, Mooney DJ. Cyclic tensile strain triggers a sequence of autocrine and paracrine signaling to regulate angiogenic sprouting in human vascular cells. Proceedings of the National Academy of Sciences. 2009; 106(36):15279–15284.
6. Paszkowiak JJ, Dardik A. Arterial wall shear stress: observations from the bench to the bedside. Vascular and endovascular surgery. 2003; 37(1):47–57. [PubMed: 12577139]
7. Leopold JA, Loscalzo J. Oxidative enzymopathies and vascular disease. Arteriosclerosis, thrombosis, and vascular biology. 2005; 25(7):1332–1340.
8. Frangos JA, Eskin SG, McIntire LV, Ives C. Flow effects on prostacyclin production by cultured human endothelial cells. Science. 1985; 227:1477–1480. [PubMed: 3883488]

9. Nigro P, Abe J-i, Berk BC. Flow shear stress and atherosclerosis: a matter of site specificity. Antioxidants & redox signaling. 2011; 15(5):1405–1414. [PubMed: 21050140]
10. Humphrey J, Rajagopal K. A constrained mixture model for growth and remodeling of soft tissues. Mathematical models and methods in applied sciences. 2002; 12(03):407–430.
11. Valentin A, Humphrey J. Evaluation of fundamental hypotheses underlying constrained mixture models of arterial growth and remodelling. Philosophical Transactions of the Royal Society of London A: Mathematical, Physical and Engineering Sciences. 2009; 367(1902):3585–3606.
12. Valentín A, Holzapfel GA. Constrained mixture models as tools for testing competing hypotheses in arterial biomechanics: a brief survey. Mechanics research communications. 2012; 42:126–133. [PubMed: 22711947]
13. Sankaran S, Humphrey JD, Marsden AL. An efficient framework for optimization and parameter sensitivity analysis in arterial growth and remodeling computations. Computer methods in applied mechanics and engineering. 2013; 256:200–210. [PubMed: 23626380]
14. Wu J, Shadden SC. Coupled simulation of hemodynamics and vascular growth and remodeling in a subject-specific geometry. Annals of biomedical engineering. 2015; 43(7):1543–1554. [PubMed: 25731141]
15. Ramachandra AB, Sankaran S, Humphrey JD, Marsden AL. Computational simulation of the adaptive capacity of vein grafts in response to increased pressure. Journal of biomechanical engineering. 2015; 137(3):031009.
16. LaDisa J, John F, Dholakia RJ, Figueroa CA, Vignon-Clementel IE, Chan FP, Samyn MM, Cava JR, Taylor CA, Feinstein JA. Computational simulations demonstrate altered wall shear stress in aortic coarctation patients treated by resection with end-to-end anastomosis. Congenital heart disease. 2011; 6(5):432–443. [PubMed: 21801315]
17. Meierhofer C, Schneider EP, Lyko C, Hutter A, Martinoff S, Markl M, Hager A, Hess J, Stern H, Fratz S. Wall shear stress and flow patterns in the ascending aorta in patients with bicuspid aortic valves differ significantly from tricuspid aortic valves: a prospective study. European Heart Journal–Cardiovascular Imaging. 2012; 14(8):797–804. [PubMed: 23230276]
18. Caro, CG. The mechanics of the circulation. Cambridge University Press; 2012.
19. Taylor CA, Draney MT. Experimental and computational methods in cardiovascular fluid mechanics. Annu Rev Fluid Mech. 2004; 36:197–231.
20. Shi Y, Lawford P, Hose R. Review of zero-d and 1-d models of blood flow in the cardiovascular system. Biomedical engineering online. 2011; 10(1):33. [PubMed: 21521508]
21. Zhang J-M, Zhong L, Su B, Wan M, Yap JS, Tham JP, Chua LP, Ghista DN, Tan RS. Perspective on cfd studies of coronary artery disease lesions and hemodynamics: A review. International journal for numerical methods in biomedical engineering. 2014; 30(6):659–680. [PubMed: 24459034]
22. Morris PD, Narracott A, von Tengg-Kobligk H, Soto DAS, Hsiao S, Lungu A, Evans P, Bressloff NW, Lawford PV, Hose DR, et al. Computational fluid dynamics modelling in cardiovascular medicine. Heart. 2016; 102(1):18–28. [PubMed: 26512019]
23. Withey DJ, Koles ZJ. A review of medical image segmentation: methods and available software. International Journal of Bioelectromagnetism. 2008; 10(3):125–148.
24. Merrill EW, Pelletier GA. Viscosity of human blood: transition from newtonian to non-newtonian. Journal of applied physiology. 1967; 23(2):178–182. [PubMed: 6040532]
25. Vignon-Clementel IE, Figueroa C, Jansen K, Taylor C. Outflow boundary conditions for 3d simulations of non-periodic blood flow and pressure fields in deformable arteries. Computer methods in biomechanics and biomedical engineering. 2010; 13(5):625–640. [PubMed: 20140798]
26. Moghadam ME, Bazilevs Y, Hsia TY, Vignon-Clementel IE, Marsden AL, et al. A comparison of outlet boundary treatments for prevention of backflow divergence with relevance to blood flow simulations. Computational Mechanics. 2011; 48(3):277–291.
27. Anor T, Grinberg L, Baek H, Madsen JR, Jayaraman MV, Karniadakis GE. Modeling of blood flow inarterial trees. Wiley Interdisciplinary Reviews: Systems Biology and Medicine. 2010; 2(5):612–623. [PubMed: 20836052]

28. Ryu J, Hu X, Shadden SC. A coupled lumped-parameter and distributed network model for cerebral pulse- wave hemodynamics. Journal of biomechanical engineering. 2015; 137(10): 101009. [PubMed: 26287937]
29. Arthurs CJ, Lau KD, Asrress KN, Redwood SR, Figueroa CA. A mathematical model of coronary blood flow control: simulation of patient-specific three-dimensional hemodynamics during exercise. American Journal of Physiology-Heart and Circulatory Physiology. 2016; 310(9):H1242–H1258. [PubMed: 26945076]
30. Grinberg, L., Insley, JA., Morozov, V., Papka, ME., Karniadakis, GE., Fedosov, D., Kumaran, K. A new com- putational paradigm in multiscale simulations: Application to brain blood flow. High Performance Computing, Networking, Storage and Analysis (SC), 2011 International Conference for; IEEE; 2011. p. 1-12.
31. Chen S, Doolen GD. Lattice boltzmann method for fluid flows. Annual review of fluid mechanics. 1998; 30(1):329–364.
32. Peters, A., Melchionna, S., Kaxiras, E., Lätt, J., Sircar, J., Bernaschi, M., Bison, M., Succi, S. Multiscale simulation of cardiovascular flows on the ibm bluegene/p: Full heart-circulation system at red-blood cell resolution. Proceedings of the 2010 ACM/IEEE International Conference for High Performance Computing, Networking, Storage and Analysis; IEEE Computer Society; 2010. p. 1-10.
33. Godenschwager, C., Schornbaum, F., Bauer, M., Köstler, H., Rüde, U. A framework for hybrid parallel flow simulations with a trillion cells in complex geometries. Proceedings of the International Conference on High Performance Computing, Networking, Storage and Analysis; ACM; 2013. p. 35
34. Randles, A., Draeger, EW., Oppelstrup, T., Krauss, L., Gunnels, JA. Massively parallel models of the human circulatory system. Proceedings of the International Conference for High Performance Computing, Networking, Storage and Analysis; ACM; 2015. p. 1
35. Xiao N, Humphrey JD, Figueroa CA. Multi-scale computational model of three-dimensional hemodynamics within a deformable full-body arterial network. Journal of computational physics. 2013; 244:22–40. [PubMed: 23729840]
36. Seo JH, Mittal R. Effect of diastolic flow patterns on the function of the left ventricle. Physics of Fluids. 2013; 25(11):110801.
37. Griffith BE. Immersed boundary model of aortic heart valve dynamics with physiological driving and loading conditions. International Journal for Numerical Methods in Biomedical Engineering. 2012; 28(3):317–345. [PubMed: 25830200]
38. Ku DN, Giddens DP, Zarins CK, Glagov S. Pulsatile flow and atherosclerosis in the human carotid bifurcation. positive correlation between plaque location and low oscillating shear stress. Arteriosclerosis, thrombosis, and vascular biology. 1985; 5(3):293–302.
39. Peiffer V, Sherwin SJ, Weinberg PD. Does low and oscillatory wall shear stress correlate spatially with early atherosclerosis? a systematic review. Cardiovascular research. 2013:cvt044.
40. Taylor CA, Fonte TA, Min JK. Computational fluid dynamics applied to cardiac computed tomography for noninvasive quantification of fractional flow reserve. Journal of the American College of Cardiology. 2013; 61(22):2233–2241. [PubMed: 23562923]
41. Steinman DA, Milner JS, Norley CJ, Lownie SP, Holdsworth DW. Image-based computational simulation of flow dynamics in a giant intracranial aneurysm. American Journal of Neuroradiology. 2003; 24(4):559– 566. [PubMed: 12695182]
42. De Leval M, Dubini G, Jalali H, Pietrabissa R, et al. Use of computational fluid dynamics in the design of surgical procedures: application to the study of competitive flows in cavopulmonary connections. The Journal of Thoracic and Cardiovascular Surgery. 1996; 111(3):502–513. [PubMed: 8601964]
43. Gounley, J., Chaudhury, R., Vardhan, M., Driscoll, M., Pathangey, G., Winarta, K., Ryan, J., Frakes, D., Randles, A. Does the degree of coarctation of the aorta influence wall shear stress focal heterogeneity?. Engineering in Medicine and Biology Society (EMBC), 2016 IEEE 38th Annual International Conference of the; IEEE; 2016. p. 3429-3432.

44. Gijsen FJ, Wentzel JJ, Thury A, Lamers B, Schuurbiers JC, Serruys PW, Van der Steen AF. A new imaging technique to study 3-d plaque and shear stress distribution in human coronary artery bifurcations in vivo. Journal of biomechanics. 2007; 40(11):2349–2357. [PubMed: 17335832]
45. Coskun AU, Yeghiazarians Y, Kinlay S, Clark ME, Ilegbusi OJ, Wahle A, Sonka M, Popma JJ, Kuntz RE, Feldman CL, et al. Reproducibility of coronary lumen, plaque, and vessel wall reconstruction and of endothelial shear stress measurements in vivo in humans. Catheterization and Cardiovascular Interventions. 2003; 60(1):67–78. [PubMed: 12929106]
46. Vorp DA, Geest JPV. Biomechanical determinants of abdominal aortic aneurysm rupture. Arteriosclerosis, thrombosis, and vascular biology. 2005; 25(8):1558–1566.
47. Boyd AJ, Kuhn DC, Lozowy RJ, Kulbisky GP. Low wall shear stress predominates at sites of abdominal aortic aneurysm rupture. Journal of vascular surgery. 2016; 63(6):1613–1619. [PubMed: 25752691]
48. Natsume K, Shiiya N, Takehara Y, Sugiyama M, Satoh H, Yamashita K, Washiyama N. Characterizing saccular aortic arch aneurysms from the geometry-flow dynamics relationship. The Journal of Thoracic and Cardiovascular Surgery. 2016
49. Cebral JR, Castro MA, Burgess JE, Pergolizzi RS, Sheridan MJ, Putman CM. Characterization of cerebral aneurysms for assessing risk of rupture by using patient-specific computational hemodynamics models. American Journal of Neuroradiology. 2005; 26(10):2550–2559. [PubMed: 16286400]
50. Ford MD, Nikolov HN, Milner JS, Lownie SP, DeMont EM, Kalata W, Loth F, Holdsworth DW, Steinman DA. Piv-measured versus cfd-predicted flow dynamics in anatomically realistic cerebral aneurysm models. Journal of biomechanical engineering. 2008; 130(2):021015. [PubMed: 18412502]
51. Baek H, Jayaraman M, Richardson P, Karniadakis G. Flow instability and wall shear stress variation in intracranial aneurysms. Journal of the Royal Society Interface. 2009:rsif20090476.
52. Dur O, Coskun ST, Coskun KO, Frakes D, Kara LB, Pekkan K. Computer-aided patient-specific coronary artery graft design improvements using cfd coupled shape optimizer. Cardiovascular engineering and technology. 2011; 2(1):35–47. [PubMed: 22448203]
53. Sengupta D, Kahn AM, Kung E, Moghadam ME, Shirinsky O, Lyskina GA, Burns JC, Marsden AL. Thrombotic risk stratification using computational modeling in patients with coronary artery aneurysms following kawasaki disease. Biomechanics and modeling in mechanobiology. 2014; 13(6):1261–1276. [PubMed: 24722951]
54. Kung E, Baretta A, Baker C, Arbia G, Biglino G, Corsini C, Schievano S, Vignon-Clementel IE, Dubini G, Pennati G, et al. Predictive modeling of the virtual hemi-fontan operation for second stage single ventricle palliation: two patient-specific cases. Journal of biomechanics. 2013; 46(2): 423–429. [PubMed: 23174419]
55. Cibis M, Jarvis K, Markl M, Rose M, Rigsby C, Barker AJ, Wentzel JJ. The effect of resolution on viscous dissipation measured with 4d flow mri in patients with fontan circulation: Evaluation using computational fluid dynamics. Journal of biomechanics. 2015; 48(12):2984–2989. [PubMed: 26298492]
56. Haggerty CM, Restrepo M, Tang E, de Zélicourt DA, Sundareswaran KS, Mirabella L, Bethel J, Whitehead KK, Fogel MA, Yoganathan AP. Fontan hemodynamics from 100 patient-specific cardiac magnetic resonance studies: a computational fluid dynamics analysis. The Journal of thoracic and cardiovascular surgery. 2014; 148(4):1481–1489. [PubMed: 24507891]
57. Marsden AL, Bazilevs Y, Long CC, Behr M. Recent advances in computational methodology for simulation of mechanical circulatory assist devices. Wiley Interdisciplinary Reviews: Systems Biology and Medicine. 2014; 6(2):169–188. [PubMed: 24449607]
58. Marsden AL, Esmaily-Moghadam M. Multiscale modeling of cardiovascular flows for clinical decision support. Applied Mechanics Reviews. 2015; 67(3):030804.
59. Nørgaard BL, Leipsic J, Gaur S, Seneviratne S, Ko BS, Ito H, Jensen JM, Mauri L, De Bruyne B, Bezerra H, et al. Diagnostic performance of noninvasive fractional flow reserve derived from coronary computed tomography angiography in suspected coronary artery disease: the nxt trial (analysis of coronary blood flow using ct angiography: Next steps). Journal of the American College of Cardiology. 2014; 63(12):1145–1155. [PubMed: 24486266]

60. Liu J, Dyverfeldt P, Acevedo-Bolton G, Hope M, Saloner D. Highly accelerated aortic 4d flow mr imaging with variable-density random undersampling. Magnetic resonance imaging. 2014; 32(8): 1012–1020. [PubMed: 24846341]

61. De Zelicourt D, Pekkan K, Kitajima H, Frakes D, Yoganathan AP. Single-step stereolithography of complex anatomical models for optical flow measurements. Transactions of the ASME-K-Journal of Biomechanical Engineering. 2005; 127(1):204–207.

62. Nair P, Chong BW, Indahlastari A, Ryan J, Workman C, Babiker MH, Farsani HY, Baccin CE, Frakes D. Hemodynamic characterization of geometric cerebral aneurysm templates treated with embolic coils. Journal of biomechanical engineering. 2016; 138(2):021011. [PubMed: 26593324]

63. Ionita, CN., Mokin, M., Varble, N., Bednarek, DR., Xiang, J., Snyder, KV., Siddiqui, AH., Levy, EI., Meng, H., Rudin, S. Challenges and limitations of patient-specific vascular phantom fabrication using 3d polyjet printing. Proceedings of SPIE–the International Society for Optical Engineering; NIH Public Access; 2014. p. 90380M

64. Ryan JR, Almefty KK, Nakaji P, Frakes DH. Cerebral aneurysm clipping surgery simulation using patient-specific 3d printing and silicone casting. World neurosurgery. 2016; 88:175–181. [PubMed: 26805698]

65. Ejaz F, Ryan J, Henriksen M, Stomski L, Feith M, Osborn M, Pophal S, Richardson R, Frakes D. Color-coded patient-specific physical models of congenital heart disease. Rapid Prototyping Journal. 2014; 20(4):336–343.

66. Costello JP, Olivieri LJ, Krieger A, Thabit O, Marshall MB, Yoo SJ, Kim PC, Jonas RA, Nath DS. Utilizing three-dimensional printing technology to assess the feasibility of high-fidelity synthetic ventricular septal defect models for simulation in medical education. World Journal for Pediatric and Congenital Heart Surgery. 2014; 5(3):421–426. [PubMed: 24958045]

67. Jacobs S, Grunert R, Mohr FW, Falk V. 3d-imaging of cardiac structures using 3d heart models for planning in heart surgery: a preliminary study. Interactive cardiovascular and thoracic surgery. 2008; 7(1):6–9. [PubMed: 17925319]

68. Ryan J, Gregg C, Frakes D, Pophal S. Three-dimensional printing: changing clinical care or just a passing fad? Current Opinion in Cardiology. 2017; 32(1):86–92. [PubMed: 27861185]

69. Costello JP, Olivieri LJ, Su L, Krieger A, Alfares F, Thabit O, Marshall MB, Yoo SJ, Kim PC, Jonas RA, et al. Incorporating three-dimensional printing into a simulation-based congenital heart disease and critical care training curriculum for resident physicians. Congenital heart disease. 2015; 10(2):185–190. [PubMed: 25385353]

70. Pedley, TJ. The fluid mechanics of large blood vessels. Vol. 1. Cambridge University Press; Cambridge: 1980.

71. Roache, PJ. Verification and validation in computational science and engineering. Hermosa Albuquerque, NM: 1998.

72. Yiallourou TI, Kröger JR, Stergiopulos N, Maintz D, Martin BA, Bunck AC. Comparison of 4d phase-contrast mri flow measurements to computational fluid dynamics simulations of cerebrospinal fluid motion in the cervical spine. PloS one. 2012; 7(12):e52284. [PubMed: 23284970]

73. Rutkowski DR, Reeder SB, Fernandez LA, Roldán-Alzate A. Surgical planning for living donor liver transplant using 4d flow mri, computational fluid dynamics and in vitro experiments. Computer Methods in Biome- chanics and Biomedical Engineering: Imaging & Visualization. 2017:1–11.

74. Kaminsky R, Dumont K, Weber H, Schroll M, Verdonck P. Piv validation of blood-heart valve leaflet interaction modelling. The International journal of artificial organs. 2007; 30(7):640–648. [PubMed: 17674341]

75. Zeng D, Ding Z, Friedman MH, Ethier CR. Effects of cardiac motion on right coronary artery hemodynamics. Annals of biomedical engineering. 2003; 31(4):420–429. [PubMed: 12723683]

76. Jung J, Lyczkowski RW, Panchal CB, Hassanein A. Multiphase hemodynamic simulation of pulsatile flow in a coronary artery. Journal of biomechanics. 2006; 39(11):2064–2073. [PubMed: 16111686]

77. Rybicki FJ, Melchionna S, Mitsouras D, Coskun AU, Whitmore AG, Steigner M, Nallamshetty L, Welt FG, Bernaschi M, Borkin M, et al. Prediction of coronary artery plaque progression and

potential rupture from 320-detector row prospectively ecg-gated single heart beat ct angiography: Lattice boltzmann evaluation of endothelial shear stress. The International Journal of Cardiovascular Imaging. 2009; 25(2):289–299. [PubMed: 19043805]

78. Bernaschi M, Bisson M, Fatica M, Melchionna S, Succi S. Petaflop hydrokinetic simulations of complex flows on massive gpu clusters. Computer Physics Communications. 2013; 184(2):329–341.
79. Choi G, Lee JM, Kim HJ, Park JB, Sankaran S, Otake H, Doh JH, Nam CW, Shin ES, Taylor CA, et al. Coronary artery axial plaque stress and its relationship with lesion geometry. JACC: Cardiovascular Imaging. 2015; 8(10):1156–1166. [PubMed: 26363834]
80. Moss E, Puskas JD, Thourani VH, Kilgo P, Chen EP, Leshnower BG, Lattouf OM, Guyton RA, Glas KE, Halkos ME. Avoiding aortic clamping during coronary artery bypass grafting reduces postoperative stroke. The Journal of thoracic and cardiovascular surgery. 2015; 149(1):175–180. [PubMed: 25293356]
81. Yamada, Y., Tsukahara, T., Motosuke, M., Fujino, Y. Cfd analysis of strut influence on blood flow in stent- implanted left main coronary artery bifurcation. Engineering in Medicine and Biology Society (EMBC), 2016 IEEE 38th Annual International Conference of the; IEEE; 2016. p. 3306-3309.
82. Xu L, Yang M, Ye L, Dong Z. Computational fluid dynamics analysis and piv validation of a bionic vortex flow pulsatile lvad. Technology and Health Care. 2015; 23(s2):S443–S451. [PubMed: 26410511]
83. Pekkan K, Whited B, Kanter K, Sharma S, De Zelicourt D, Sundareswaran K, Frakes D, Rossignac J, Yoganathan AP. Patient-specific surgical planning and hemodynamic computational fluid dynamics optimization through free-form haptic anatomy editing tool (surgem). Medical & biological engineering & computing. 2008; 46(11):1139–1152. [PubMed: 18679735]
84. Marsden AL, Bernstein AJ, Reddy VM, Shadden SC, Spilker RL, Chan FP, Taylor CA, Feinstein JA. Evaluation of a novel y-shaped extracardiac fontan baffle using computational fluid dynamics. The Journal of Thoracic and Cardiovascular Surgery. 2009; 137(2):394–403. [PubMed: 19185159]
85. Yang W, Feinstein JA, Marsden AL. Constrained optimization of an idealized y-shaped baffle for the fontan surgery at rest and exercise. Computer methods in applied mechanics and engineering. 2010; 199(33):2135–2149.
86. Samuelson R, Nair P, Snyder K, Frakes D, Preul MC, Nakaji P, Spetzler RF. Fluid dynamic characteri- zation of a novel branching anastomosis design. International Biomechanics. 2015; 2(1):73–78.
87. LaDisa JF, Olson LE, Guler I, Hettrick DA, Audi SH, Kersten JR, Warltier DC, Pagel PS. Stent design properties and deployment ratio influence indexes of wall shear stress: a three-dimensional computational fluid dynamics investigation within a normal artery. Journal of Applied Physiology. 2004; 97(1):424–430. [PubMed: 14766776]
88. Bressloff NW, Ragkousis G, Curzen N. Design optimisation of coronary artery stent systems. Annals of biomedical engineering. 2016; 44(2):357–367. [PubMed: 26183960]
89. Zhang M, Anzai H, Chopard B, Ohta M. Towards the patient-specific design of flow diverters made from helix-like wires: an optimization study. BioMedical Engineering OnLine. 2016; 15(2): 371.
90. Suzuki, T., Takao, H., Fujimura, S., Dahmani, C., Ishibashi, T., Mamori, H., Fukushima, N., Yamamoto, M., Murayama, Y. Selection of helical braided flow diverter stents based on hemodynamic performance and mechanical properties. Journal of neurointerventional surgery. 2016. DOI http://dx.doi.org/10.1136/neurintsurg-2016--12561
91. Chung B, Cebral JR. Cfd for evaluation and treatment planning of aneurysms: review of proposed clinical uses and their challenges. Annals of biomedical engineering. 2015; 43(1):122–138. [PubMed: 25186432]
92. Walcott BP, Reinshagen C, Stapleton CJ, Choudhri O, Rayz V, Saloner D, Lawton MT. Predictive modeling and in vivo assessment of cerebral blood flow in the management of complex cerebral aneurysms. Journal of Cerebral Blood Flow & Metabolism. 2016; 36(6):998–1003. [PubMed: 27009946]

93. LaDisa JF, Taylor CA, Feinstein JA. Aortic coarctation: recent developments in experimental and computational methods to assess treatments for this simple condition. Progress in pediatric cardiology. 2010; 30(1):45–49. [PubMed: 21152106]

94. Cosentino D, Capelli C, Derrick G, Khambadkone S, Muthurangu V, Taylor AM, Schievano S. Patient- specific computational models to support interventional procedures: a case study of complex aortic re-coarctation. EuroIntervention. 2015; 11(5):669–672. [PubMed: 26348674]

95. Marsden AL. Simulation based planning of surgical interventions in pediatric cardiology. Physics of Fluids. 2013; 25(10):101303. [PubMed: 24255590]

96. Randles, AP., Kale, V., Hammond, J., Gropp, W., Kaxiras, E. Performance analysis of the lattice boltzmann model beyond navier-stokes. Parallel & Distributed Processing (IPDPS), 2013 IEEE 27th International Symposium on; IEEE; 2013. p. 1063-1074.

97. Bernaschi M, Melchionna S, Succi S, Fyta M, Kaxiras E, Sircar JK. Muphy: A parallel multi physics/scale code for high performance bio-fluidic simulations. Computer Physics Communications. 2009; 180(9):1495–1502.

Trends

The improved capabilities of additive manufacturing in terms of material properties and resolution is opening new and exciting possibilities for the use of 3D printing in cardiovascular medicine.

Methods for using high performance computing to enable high fidelity and patient-specific fluid simulations are rapidly evolving, providing new insights into the role hemodynamic forces play in cardiovascular disease.

The emerging synergy between large-scale simulations and 3D printing is having a two-fold benefit: 1) 3D printing can be used to validate the complex simulations and 2) the flow models can be used to improve treatment planning for cardiovascular disease.

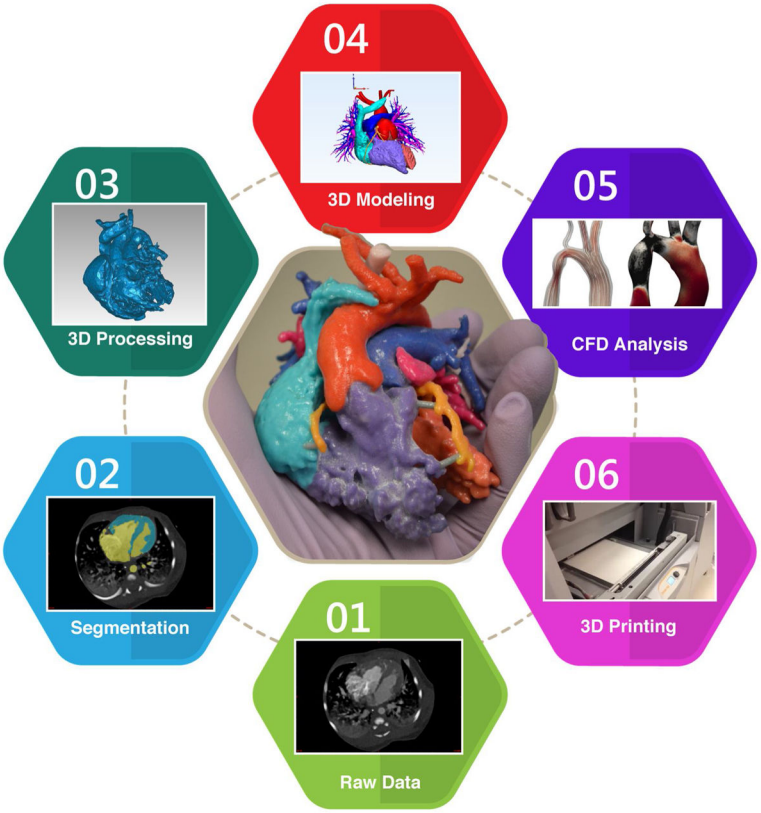

Figure 1.
Schematic of the process moving from medical imaging to computational fluid dynamics and 3D printed models.

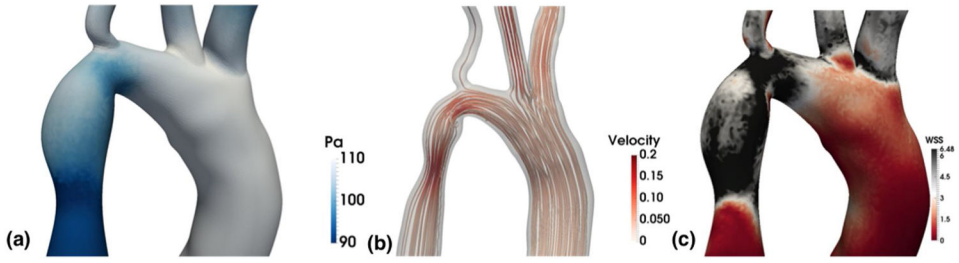

Figure 2.

Results from CFD software for hemodynamics modeled as a Newtonian fluid in an image-derived vascular geometry of a coarcted human aorta. (a) The left panel shows a pressure map. (b) The middle panel demonstrates velocity flow lines. (c) The right panel shows a wall shear stress map.

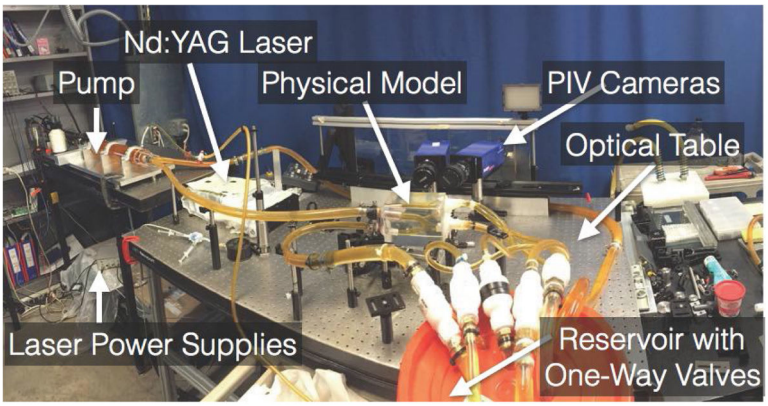

Figure 3.
Photograph of an *in vitro* flow loop. Image reproduced with permission from [43].

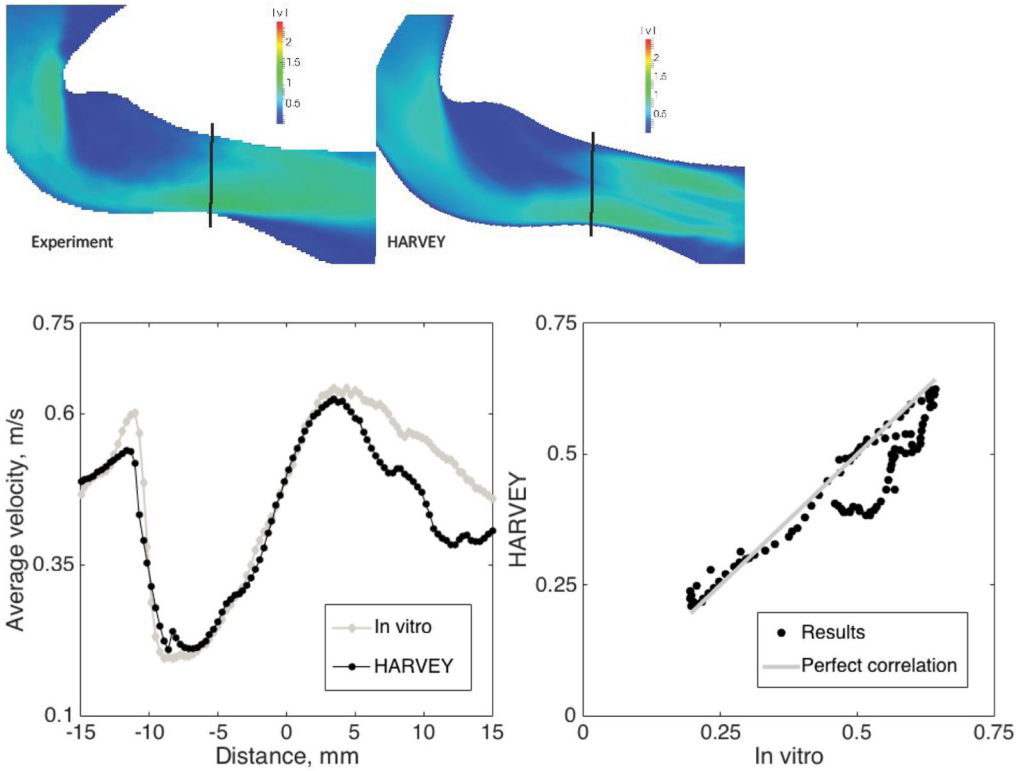

Figure 4.

Magnitude of velocity through coarctation, from *in vitro* experiment compared to HARVEY (left). In the two graphs on the right, average velocity over vertical slices of the images along the vessel is shown first, followed by a direct comparison of simulation values to *in vitro* measurements on the right. Image reproduced with permission from [43].

Table 1

Popular mesh reconstruction software packages.

Software Package	Open Source	Reference
3D Slicer	Y	https://www.slicer.org
Avizo	N	https://www.fei.com/software/amira-avizo/
Embodi 3D	Y	https://www.embodi3d.com/democratiz3D/
ITK Snap	Y	https://http://www.itksnap.org/
Mimics	N	http://www.materialise.com/en/medical/software/mimics
SCAN IP	N	https://www.simpleware.com/software/
SimVascular	Y	https://simvascular.github.io/
Terarecon	N	https://www.terarecon.com/
Vitrea	N	https://vitalimages.com

Table 2

Common computational fluid dynamics software packages for simulating 3D hemodynamics in patient-derived geometries.

Software Package	Method	FSI	Open Source	Reference
ABAQUS	FE	Y	N	https://3ds.com
COMSOL	FE	Y	N	https://www.comsol.com
CRIMSON	FE	Y	N	http://www.crimson.software
FLUENT	FE	Y	N	http://www.ansys.com
HARVEY	LB	Y	N	[96]
HemeLB	LB	N	Y	https://github.com/UCL/hemelb
IBAMR	FE	Y	Y	https://github.com/IBAMR
MUPHY	LB	Y*	N	[97]
NEK5000	FE	Y	Y	https://nek5000.mcs.anl.gov/
NEKTAR	FE	Y	Y	https://nektar.info
OPENFOAM	FV	Y	Y	https://www.openfoam.com
SimVascular	FE	Y	Y	https://simvascular.github.io/
WaLBerla	LB	Y	Y	https://www.walberla.net/

FE: finite element, FV: finite volume, LB: lattice Boltzmann.

*includes explicit cells but rigid walls.

Table 3

Forms of additive manufacturing, commonly known as 3D printing.

Process*	**Example Media****	**Technology**	**Basic Description**
Binder Jetting	Gypsum Printing	Inkjet	Liquid agents are applied to powder media selectively, in an inkjet (or inket-like) process
Material Jetting	Photopolymer	Polyjet	Photopolymer liquid is deposited on a build platform and exposed to a light source for curing
Powder Bed Fusion	Nylon	Selective laser sintering, electron beam melting	Powder materials are melted together via a high-energy heat source
Directed Energy Deposition	Metals	Laser engineered net shaping	Media is media onto a build platform while being heated by a high energy heat source
Sheet Lamination	Paper, plastic, metal film	Laminated object manufacturing	Material sheets are selectively cut and laminated together
Vat Photopolymerization	Photopolymer	Stereolithography	A vat of photopolymer liquid is selectively exposed to a light source
Material Extrusion	Plastic (ABS, PLA)	Fused deposition (fused filament fabrication)	Media is heated to a glass transition temperature and selectively deposited on a build platform

* The nomenclature presented here is developed by ASTM International.

** These examples of media and technologies are intended to be a representation of the field, but not exhaustive.